J. Phys. Chem. A **2004,** *108,* 1448−1459

Gas-Phase Reactions between Silane and Water: A Theoretical Study

Shao-Wen Hu,* Yi Wang, Xiang-Yun Wang, Tai-Wei Chu, and Xin-Qi Liu

Department of Applied Chemistry, College of Chemistry and Molecular Engineering, Peking University, Beijing, China 100871

Received: September 22, 2003; In Final Form: December 27, 2003

Gas-phase reactions between silane (SiH_4) and water (H_2O) were investigated using ab initio calculations at the CCSD(T)/6-311++G**//MP2/6-31+G* level. Within the energy range of 160 kcal/mol, we located 40 equilibrium and 27 transition states on the potential energy surfaces of the Si−O−H systems. Over an energy barrier of 46.61 kcal/mol, the weakly bonded molecular complex SiH_4-H_2O can eliminate first H_2 molecule and produce silanol (SiH_3OH). The transition state is a dihydrogen-bonded structure with retention of the silane configuration. The total energy of the direct products $SiH_3OH + H_2$ is −10.83 kcal/mol relative to the reactants. Over an energy barrier of 58.09 kcal/mol, SiH_4-H_2O can eliminate first H_2 and produce a transient dative bonded complex SiH_2-H_2O. Providing more energy to the system, SiH_4-H_2O can dissociate atomically and the initial products can further eliminate H_2 or H, producing smaller species including molecules SiH−OH, SiH_2-O, $Si-H_2O$, and SiO and radicals SiH_2-OH, $SiH-H_2O$, HSiO, and HOSi.

I. Introduction

Silane is used as source gas to prepare silicon-containing materials. The structure of products, varying for different applications, can be monitored through fabricating conditions. To induce SiH_4 decomposition at the gas phase, an elevated temperature is required. During the process, water is involved not only as an impurity but also as a reactant or byproduct.[1−14] At relative low temperatures, silane hydrolysis can be catalyzed by acid or base. In particular, hydrolysis of halogen or oxygen derivatives of silane results in polymeric silicones, which are precursors of sol−gel process, a widely used technique in preparing nanoscale organic and inorganic hybrids.[15−22] Clearly, understanding the reactivity of silane toward water at various temperatures is of fundamental importance and highly desired for product-quality-control. Several experimental and theoretical mechanism studies use some kind of silane derivative and water as starting reactants.[23−27] Compared to these substituted silane, how pure SiH_4 reacts with H_2O is much less known. This is probably because SiH_4 is not easy to hydrolysis in water without catalysts. The usual inertness implies that substantial energy is necessary to initiate the reactions between SiH_4 and H_2O. At such conditions, the proportion of relevant products may also be highly temperature dependent. To elucidate the unclear mechanism, the present computational work intends to explore pathways started from $SiH_4/H_2O = 1:1$ to all stoichiomically possible products within energy range of 160 kcal/mol.

II. Calculation Method

The geometry structures were fully optimized at the MP2=Full/6-31+G* level. Transition states were located using synchronous transit-guided quasi-Newton (STQN) methods [28] in combination with stepwise partial optimization along each pathway with one geometric parameter fixed as constant. Frequency calculations were performed following each optimization to obtain the zero-point energy (ZPE) and to characterize all of the stationary points located on the potential energy surface. Intrinsic reaction coordinate (IRC) calculations were performed to confirm the relationship of each transition state with its reactant and product. Single-point calculations at the MP2=Full/6-311++G** and the CCSD(T)=Full/6-311++G**levels were performed to determine the electronic energies. The relative energies reported in discussion are obtained at the CCSD(T)=Full/6-311++G** level with MP2/6-31+G* calculated ZPE corrections. For open shell species, the geometry optimization and energy calculation were performed using same level of theories except that electron spins were unrestricted. Guassian 98 program package [29] was employed for these calculations.

III. Results and Discussions

Energies calculated at three different theoretical levels were listed together with dipole moments and rotational constants for all of the species in Table 1. For open shell species using spin-unrestricted methods, spin squared expectation values $\langle S^2\rangle$ were also listed to assess spin contamination. It can be seen that using a larger basis set (6-311++G** instead of 6-31+G*) lowers the electronic energies significantly, whereas using a method that includes more effective electron correlation (CCSD instead of MP2) has a less impact. Generally, relative energies calculated at the MP2/6-311++G** level are quite close to those calculated at the CCSD (T)/6-311++G** level.

The species were named according to their structures and numbered to indicate the order of their occurrence in the reaction courses. Symbols ‘3′ or ‘TS′ were added to specify triplet state or transition state species.

Reaction pathways were divided into eight parts. Each part includes geometry structures of the relevant species and their relative energies (Figures 1−8).

Part I: Pathways from $SiH_4 + H_2O$ to SiH_3OH (4) and SiH_2-H_2O (6). At the initial stage, SiH_4 associates with H_2O

---

* To whom correspondence should be addressed. E-mail: sw-hu@163.com.

10.1021/jp036836g CCC: $27.50

TABLE 1: Electronic Energies, Dipole Moments, and Rotational Constants of the Species

		(a.u.)			(kcal/mol)		(Debye)			(GHZ)		
species	symm[a]	E_e[b]	E_e[c]	E_e[d]	ZPE[b]	$\langle S^2 \rangle$[d]	D[b]	D[c]	D[d]	rotational constants[b]		
SiH_4-H_2O(**1**)	C_1(0)	−367.526126	−367.793316	-367.837462	34.68		2.787	2.637	2.752	70.30	4.063	4.024
SiH_3-H_2-OH_TS(**2**)	C_1(1)	−367.447633	−367.718494	-367.760753	33.16		2.219	2.100	2.159	49.49	10.23	9.645
SiH_3OH-H_2(**3**)	C_s(0)	−367.551596	−367.808436	-367.850516	32.20		1.750	1.678	1.802	32.80	8.97	7.671
SiH_3OH(**4**)	C_s(0)	−366.406591	−366.646695	-366.680644	24.60		1.621	1.556	1.654	76.98	13.40	13.14
SiH_2-H-OH_TS(**5**)	C_1(1)	−366.274310	−366.516311	-366.552094	21.95		1.758	1.636	1.649	83.62	10.79	10.56
SiH_2-H_2O(**6**)	C_1(0)	−366.311327	−366.555894	-366.594574	25.08		4.557	4.350	4.470	83.36	9.141	9.063
$H_2-SiH_2-H_2O$(**7**)	C_1(0)	−367.455888	−367.717019	-367.763790	32.22		4.480	4.293	4.407	61.56	5.964	5.798
$H_2-SiH_2-H_2O$_TS(**8**)	C_s(1)	−367.421593	−367.693900	-367.740902	32.18		2.740	2.719	2.706	80.46	4.737	4.638
SiH_2_H_2O_TS(**9**)	C_s(1)	−366.308877	−366.553347	-366.592140	24.88		4.206	4.085	4.122	82.96	9.023	8.802
$H-SiH_3-H_2O$_3(**10**)	C_s(0)	−367.391536	−367.649062	-367.688721	28.38	2.001	2.856	2.717	2.846	22.38	3.711	3.361
SiH_3-H_2O(**11**)	C_s(0)	−366.893229	−367.149236	-367.188893	28.30	0.751	2.931	2.785	2.922	96.33	4.247	4.134
SiH_3-H-OH_TS(**12**)	C_1(1)	−366.832036	−367.084485	-367.136873	27.56	0.754	1.616	1.501	1.815	70.54	8.342	8.253
SiH_4-OH(**13**)	C_s(0)	−366.844585	−367.096809	-367.145936	26.28	0.751	2.144	2.023	2.114	79.64	3.792	3.781
SiH_4-H-OH_3(**14**)	C_1(0)	−367.343048	−367.596683	-367.645826	26.48	2.001	2.145	2.024	2.116	22.98	3.583	3.230
$SiH-H_2-OH$_TS(**15**)	C_1(1)	−366.270066	−366.518431	-366.555141	22.56		1.563	1.535	1.483	74.27	11.34	11.07
$SiH-OH-H_2$(**16**)	C_1(0)	−366.337008	−366.571899	-366.610059	20.76		1.330	1.403	1.348	42.91	9.947	8.083
$SiH-OH$(**17**)	C_s(0)	−365.191998	−365.411557	-365.440174	13.20		1.225	1.304	1.218	175.3	15.77	14.47
$SiH-OH$_TS(**18**)	C_1(1)	−365.175553	−365.394882	-365.424932	11.45		1.633	1.504	1.505	206.1	15.42	14.55
$SiH-OH_c$(**19**)	C_s(0)	−365.191150	−365.409564	-365.439733	12.95		1.939	1.688	1.867	172.3	15.78	14.46
$SiH-OH_c$-H_2(**20**)	C_1(0)	−366.336088	−366.571254	-366.609568	20.55		2.031	1.781	1.990	47.12	9.724	8.072
$SiH_2-H_2-OH_c$_TS(**21**)	C_1(1)	−366.269043	−366.517574	-366.554367	22.39		2.131	1.878	2.043	73.79	11.28	11.03
$SiH-OH$_3(**22**)	C_1(0)	−365.136035	−365.352799	-365.377878	12.54	2.001	1.603	1.553	1.675	217.4	14.97	14.55
$SiH-H-O$_3_TS(**23**)	C_1(1)	−365.054347	−365.268979	-365.307173	9.02	2.023	2.809	2.842	2.767	164.3	16.48	16.38
SiH_2-O_3(**24**)	C_s(0)	−365.091181	−365.303458	-365.341229	10.85	2.003	1.857	1.866	2.072	125.1	15.46	14.52
SiH_2-O(**25**)	C_{2v}(0)	−365.199321	−365.411799	-365.435032	11.86		3.866	3.765	4.799	166.9	17.89	16.16
$SiH-H-O$_TS(**26**)	C_1(1)	−365.102487	−365.316496	-365.339961	8.91		2.530	2.434	3.410	156.2	17.33	15.60
SiH_2-H_2-O_TS(**27**)	C_1(1)	−366.290409	−366.532575	-366.562927	21.50		3.438	3.337	3.970	65.75	15.22	14.45
SiH_2-O-H_2(**28**)	C_1(0)	−366.344624	−366.573486	-366.604827	19.49		4.083	4.004	5.083	164.0	8.406	8.010
$H_2-SiH-OH$_TS(**29**)	C_1(1)	−366.286565	−366.531262	-366.569906	21.73		1.379	1.433	1.432	73.37	13.26	12.88
H2−SiH−OH(**30**)	C_1(0)	−366.336462	−366.571064	-366.609186	20.18		1.202	1.275	1.188	20.80	12.36	8.493
$H_2-SiH-OH_c$_TS(**31**)	C_1(1)	−366.286902	−366.531876	-366.570646	21.64		1.791	1.588	1.710	72.03	13.30	12.89
$H_2-SiH-OH_c$(**32**)	C_1(0)	−366.335661	−366.570585	-366.608858	20.05		1.948	1.701	1.882	22.13	12.18	8.644
$Si-H_2-O$_TS(**33**)	C_s(1)	−365.117238	−365.3404f	-365.366244	9.51		2.241	2.219	2.821	113.1	18.39	15.82
SiO_H_2(**34**)	C_s(0)	−365.206860	−365.414724	-365.438939	9.14		3.200	3.214	4.299	557.1	9.155	9.007
SiO(**35**)	$C_{\infty v}$(0)	−364.061762	−364.253178	-364.269226	1.66		3.036	3.028	4.075	0.000	20.70	20.70
SiH_3-OH_3(**36**)	C_s(0)	−366.211172	−366.452203	-366.496830	19.88	2.002	2.065	1.908	1.955	78.57	3.844	3.833
$H-SiH_2-OH$_3(**37**)	C_1(0)	−366.270683	−366.500693	-366.530447	18.49	2.000	1.594	1.578	1.722	26.38	12.59	9.586
SiH_2-OH(**38**)	C_1(0)	−365.772255	−366.000764	-366.030494	18.39	0.750	1.619	1.576	1.721	111.7	14.56	13.52
$SiH-H_2-O$_TS(**39**)	C_1(1)	−365.663549	−365.894654	-365.922910	15.36	0.758	3.182	3.122	3.688	83.55	16.70	15.12
$HSiO-H_2$(**40**)	C_s(0)	−365.724628	−365.942150	-365.970915	13.31	0.757	3.761	3.726	4.809	294.0	8.432	8.202
HSiO(**41**)	C_s(0)	−364.579365	−364.780583	-364.801287	5.81	0.757	3.599	3.555	4.566	334.6	19.05	18.02
HSiO−H_3(**42**)	C_1(0)	−365.077734	−365.280527	-365.301243	5.91	2.007	3.575	3.586	4.613	270.9	10.73	10.32
HSiO−H_3_TS(**43**)	C_1(1)	−365.035471	−365.245826	-365.287176	7.28	2.180	4.173	5.092	2.259	214.3	16.33	16.04
SiH_2-H_2-OH_TS(**44**)	C_1(1)	−366.820192	−367.079075	-367.116878	27.12	0.752	1.664	1.598	1.646	68.17	10.13	9.867
SiH_2-OH-H_2(**45**)	C_1(0)	−366.917219	−367.162466	-367.200323	25.93	0.750	1.735	1.684	1.855	35.10	9.596	7.886
$H-SiH_2-H_2O$_TS(**46**)	C_s(1)	−366.809184	−367.055459	-367.095744	25.46	0.792	4.576	4.435	4.592	83.39	7.471	7.422
$H-SiH_2-H_2O$(**47**)	C_s(0)	−366.809901	−367.055849	-367.094582	25.32	0.750	4.492	4.332	4.452	74.06	6.947	6.838
SiH_2-H_2O_3(**48**)	C_s(0)	−366.263601	−366.508319	-366.543109	22.00	2.001	2.512	2.276	2.282	111.4	3.812	3.687
$H-SiH-H_2O$_3(**49**)	C_1(0)	−366.201194	−366.435592	-366.470150	19.68	2.010	4.464	4.258	4.356	37.23	8.152	6.769
$SiH-H_2O$(**50**)	C_1(0)	−365.702596	−365.935578	-365.970091	19.41	0.760	4.420	4.223	4.325	132.7	9.304	8.794
$SiH-H-OH_c$_TS(**51**)	C_1(1)	−365.660248	−365.890750	-365.927878	15.95	0.824	2.137	1.904	1.970	118.5	12.11	11.58
$SiH-H-OH$_TS(**52**)	C_1(1)	−365.658793	−365.889415	-365.926751	16.08	0.820	1.521	1.494	1.523	118.4	12.14	11.68
$Si-H_2-OH$_TS(**53**)	C_1(1)	−365.661916	−365.898826	-365.931387	16.66	0.761	1.868	1.724	1.763	109.3	11.96	11.09
$HOSi-H_2$(**54**)	C_1(0)	−365.734141	−365.957158	-365.990301	15.19	0.756	1.731	1.637	1.679	51.27	10.09	8.430
HOSi(**55**)	C_s(0)	−364.589255	−364.795542	-364.820526	7.65	0.756	1.652	1.561	1.575	771.6	16.13	15.80
Si−H−O_TS(**56**)	C_s(1)	−364.519954	−364.725543	-364.758475	3.94	0.777	2.442	2.508	2.267	326.1	19.17	18.11
H−SiO_TS(**57**)	C_s(1)	−364.553910	−364.749191	-364.770176	2.10	0.797	3.148	3.171	4.165	131.8	18.99	16.60
H−SiO(**58**)	C_s(0)	−364.560229	−364.753023	-364.769084	1.75	0.750	3.060	3.034	4.082	51.56	14.14	11.10
SiO(T)(**59**)	C^*v(0)	−363.898887	−364.089961	-364.109350	3.57	2.013	5.034	5.755	3.785	0.000	21.69	21.69
Si−H−OH_TS(**60**)	C_s(1)	−365.045970	−365.267177	-365.300205	10.80		2.291	2.046	2.286	297.0	11.05	10.89
$Si-H_2O$(**61**)	C_s(0)	−365.065131	−365.286621	-365.320763	14.68		4.961	4.769	5.003	388.6	10.15	9.895
$Si-H_2O$_3(**62**)	C_1(0)	−365.106213	−365.327159	-365.356018	14.87	2.016	4.184	3.994	4.174	319.5	8.743	8.611
Si−H−OH_3_TS(**63**)	C_1(1)	−365.058250	−365.276856	-365.308843	10.73	2.040	1.900	1.745	1.871	240.2	12.62	12.40
HOSi−H_3_TS(**64**)	C_1(1)	−365.087069	−365.295732	-365.322437	8.51	2.030	1.638	1.536	1.554	80.65	14.92	13.02
HOSi−H_3(**65**)	C_1(0)	−365.087781	−365.295496	-365.320510	7.93	2.006	1.653	1.556	1.571	34.47	14.65	10.56
HOSi−H(**66**)	C_1(0)	−365.036152	−365.251045	-365.317060	10.57		1.813	2.256	4.630	280.6	13.47	12.85
HOSi−H_TS(**67**)	C_s(1)	−365.023755	−365.242377	-365.294006	10.06		1.265	1.448	3.419	341.1	13.45	12.94
SiH_4	T_d(0)	−291.314239	−291.496687	−291.528702	20.34		0.000	0.000	0.000	85.71	85.71	85.71
SiH_3	C_{3v}(0)	−290.681414	−290.852725	-290.880244	13.91	0.751	0.142	0.168	0.212	141.8	141.8	83.72
SiH_2(T)	C_{2v}(0)	−290.053181	−290.213078	-290.235566	7.96	2.001	0.183	0.265	0.372	467.9	155.2	116.5
SiO	$C_{\infty v}$ (0)	−364.061762	−364.253178	-364.269226	1.66		3.036	3.028	4.075	0.000	20.70	20.70
H_2O	C_{2v}(0)	−76.208623	−76.293534	-76.305516	13.30		2.329	2.171	2.238	817.7	419.6	277.3
HO	$C_{\infty v}$ (0)	−75.528599	−75.598387	-75.615332	5.28	0.751	1.958	1.846	1.919	0.000	553.5	553.5
H_2	$D_{\infty h}$(0)	−1.144141	−1.160301	-1.168352	6.48		0.000	0.000	0.000	0.000	1842	1842
H		−0.498233	−0.499818	-0.499818								

[a] Symmetry of the species, the number of imaginary frequency are in parentheses. [b] MP2/6-31+G*// MP2/6-31+G* calculations. [c] MP2/6-311++G**// MP2/6-31+G* calculations. [d] CCSD(T)/6-311++G**// MP2/6-31+G* calculations.

through a weak bond as shown by the structure of molecular complex SiH_4-H_2O (**1**). The association, with binding energy of 1.00 kcal/mol, changes the Si−H bond length slightly. In the following discussion, we use **1** as the initial reactant of the

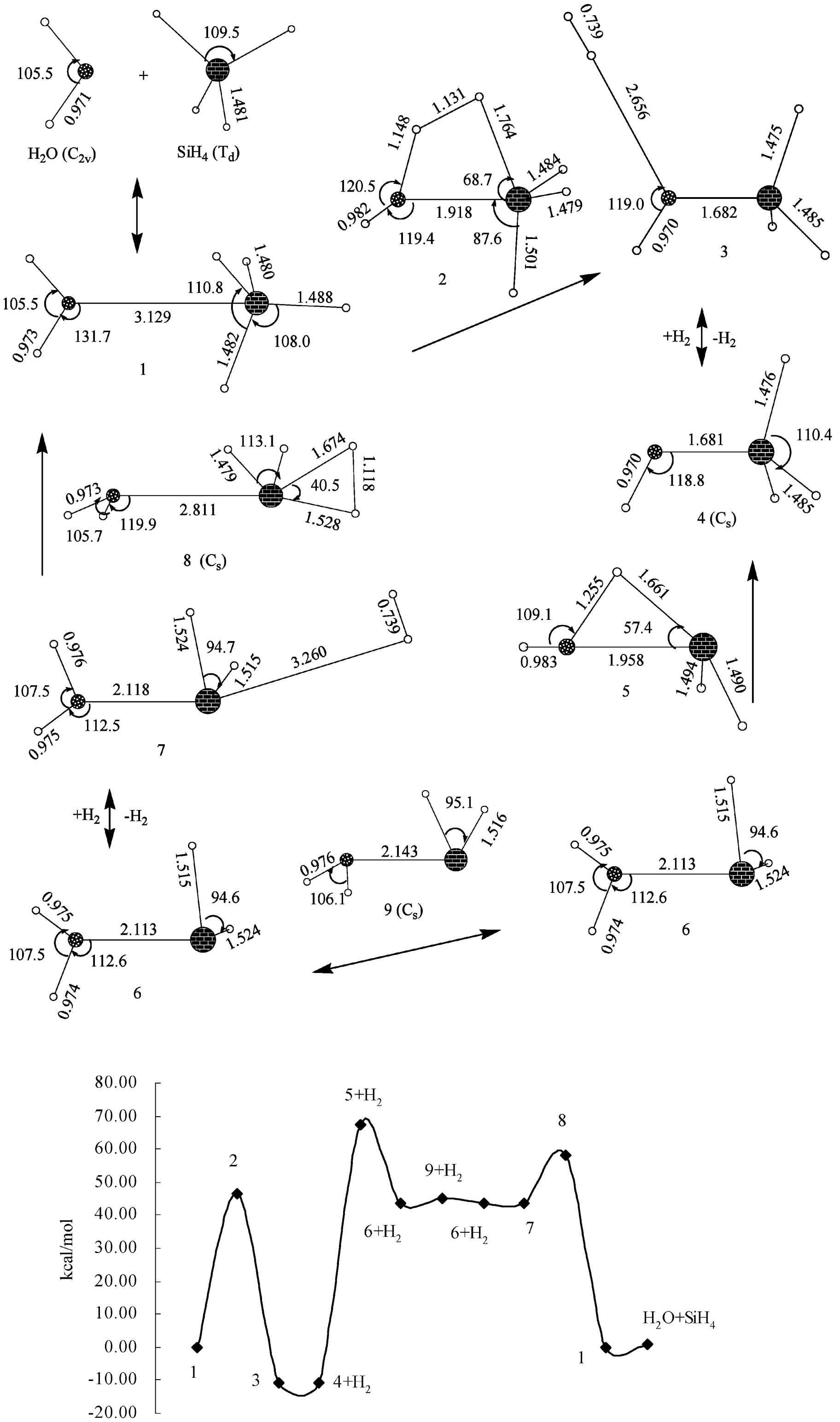

Figure 1. Species involved in H_2 elimination from SiH_4−H_2O (**1**). Bond lengths are in Å, and angles are in degrees. The species beside arrows are transition states or H_2. The direction of arrows is toward energy descent; the relative energy of SiH_4-H_2O(**1**) is 0.00 kcal/mol. The symmetry for the species is in parentheses but C_1 is omitted.

total system and set its relative energy as 0.00 kcal/mol. From our point of view, this is a better choice to circumvent basis set superposition error (BSSE), because in **1**, the SiH_4 and H_2O groups can use each other's basis sets as most of the associated species, but the separated SiH_4 and H_2O can only use their own basis sets.

With 46.61 kcal/mol energy, the system can be activated from **1** to transition state SiH_2−H_2−OH−TS (**2**), a ring structure formed through a dihydrogen bond −H−H− and a Si−O bond. To form the −H−H− bond, the positive partial charged H from H_2O associates with the negative partial charged H from SiH_4. The hydrogen molecule produced from the −H−H− bond then eliminates and results in SiH_3OH−H_2 (**3**), a molecular combination of silanol SiH_3OH (**4**) and H_2. It can be seen that silanol produced in this way retains three original hydrogen atoms bonded to silicon in SiH_4, only one of the hydrogen atoms is

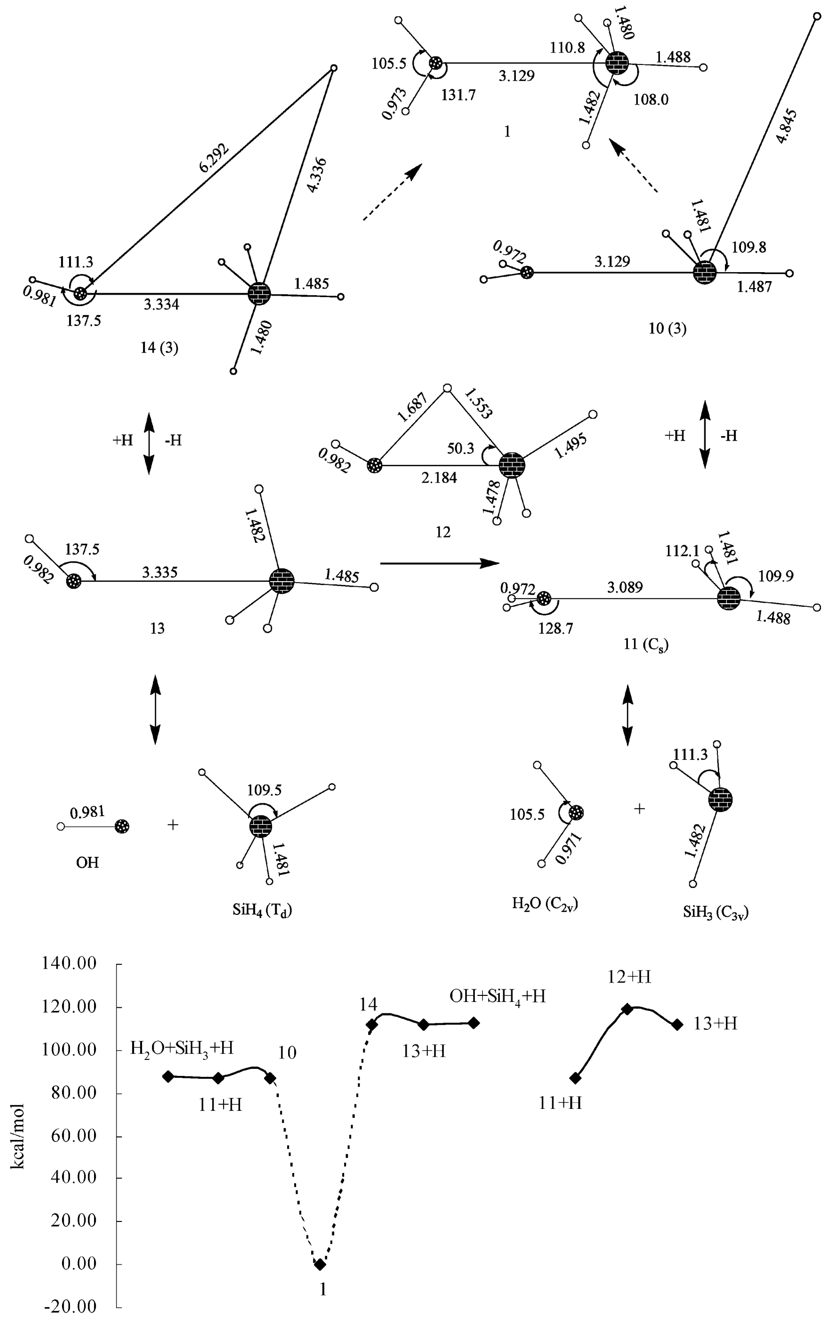

Figure 2. Species involved in H elimination from SiH_4-H_2O (**1**). Bond lengths are in Å, and angles are in degrees. The species beside arrows are transition states or H. The direction of arrows is toward energy descent. The dashed lines or arrows indicate triplet−singlet transitions. The relative energy of SiH_4-H_2O (**1**) is 0.00 kcal/mol. In parentheses, triplet species are labeled "3" and symmetry of the species are indicated except for C_1.

replaced by an OH group. The energy of **3** is −10.67 kcal/mol relative to **1**, indicating the process is thermodynamically favored. A similar mechanism has been proposed to interpret the hydrohalogen HX (X = Cl or F) elimination as halosilanes are attacked by water.[25−27] Compared to Si−Cl or Si−F, the Si−H bond is less polarized, so it has a smaller tendency to associate with proton-like hydrogen from H_2O. As a result, the energy barrier of H_2 elimination is considerable higher than that of HX elimination. This is perhaps the reason that halosilanes but not pure SiH_4 are usually used as source material for hydrolytic applications.

Alternatively, SiH_4 is known to dissociate into SiH_2 and H_2 at elevated temperature, a process that proceeds a little easier if a Lewis base is around.[30,31] With 58.09 kcal/mol energy, the SiH_4/H_2O system can be activated to the transition state $H_2-SiH_2-H_2O$_TS (**8**). The barrier is slightly less than that required for SiH_4 self-dissociation,[31] indicating the weak Lewis base character of H_2O. The Si−O distance shortens as H_2 eliminates until a dative bond forms as shown from **1** to **8** to $H_2-SiH_2-H_2O$ (**7**). In **7**, the donor−acceptor complex SiH_2-H_2O (**6**) and H_2 are loosely combined. SiH_2 is a much stronger Lewis acid than SiH_4, it draws weak Lewis base H_2O closer in **6** than SiH_4 does in **1**. The structure of **6** prefers asymmetric configuration. The barrier (1.32 kcal/mol) between the two enantiomers of **6**, as shown by transition state SiH_2-H_2O_TS (**9**), is too small to show chirality of the species. Relative to its covalent bonded isomer **4**, the energy of the dative bonded **6** is 54.49 kcal/mol. The barrier from **6** to **4** is 23.52 kcal/mol, higher than that from **7** to **1** (14.32 kcal/mol). Thus, if the H_2 molecule is not fully eliminated, backward reaction from **7** to **1** is more likely to happen. As shown by the structures of **6**, transition state SiH_2-H-OH_TS (**5**), and **4**, one of the three hydrogen atoms bonded

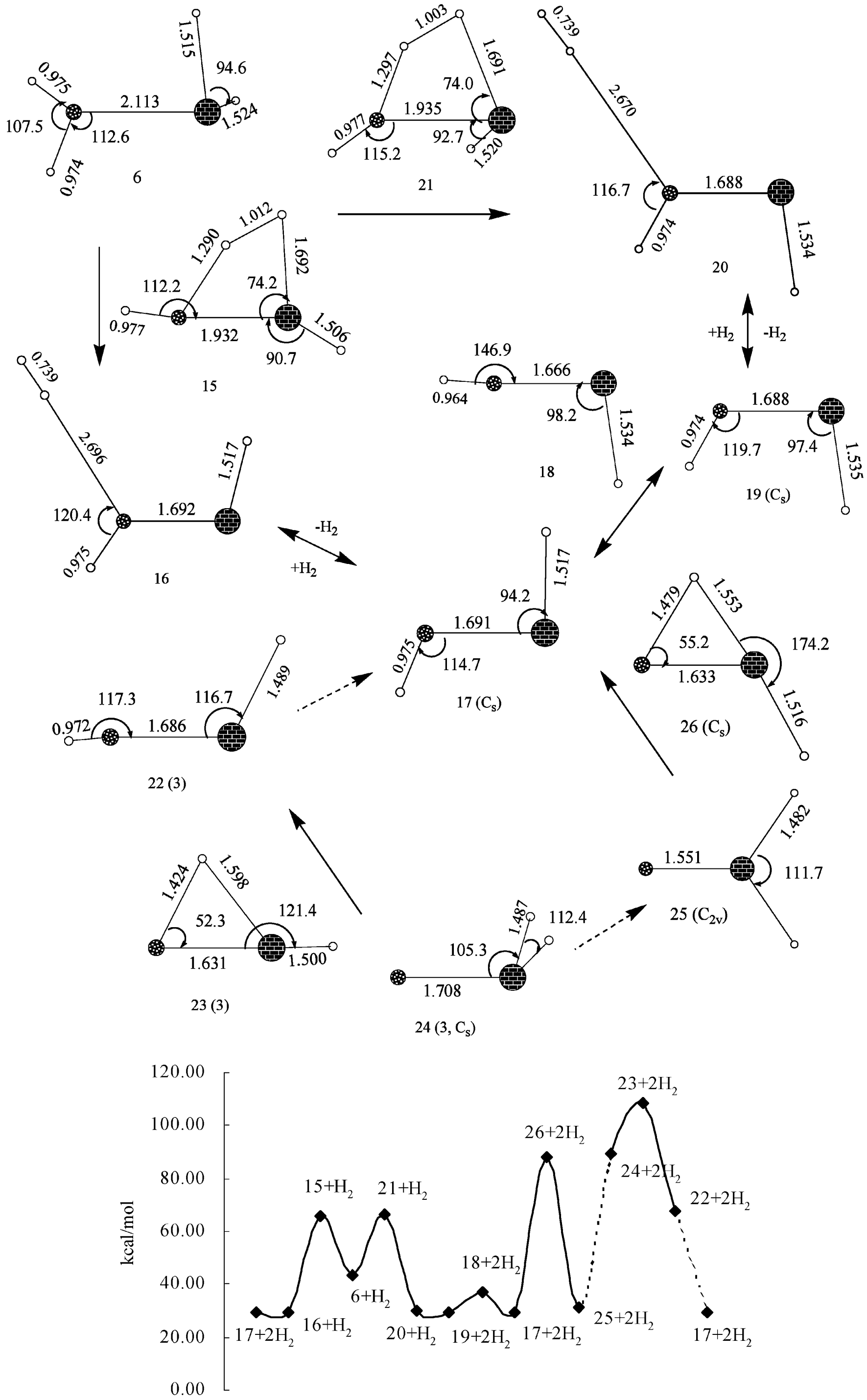

Figure 3. Species involved in H_2 elimination from H_2O-SiH_2 (**6**). Bond lengths are in Å, and angles are in degrees. The species beside arrows are transition states or H_2. The direction of arrows is toward energy descent. The dashed lines or arrows indicate triplet−singlet transitions. The relative energy of SiH_4-H_2O (**1**) is 0.00 kcal/mol. In parentheses, triplet species are labeled "3" and symmetry of the species are indicated except for C_1.

to silicon in **4** comes from H_2O. Therefore, the two routes toward **4** may be distinguished experimentally by examining whether the hydrogen atoms bonded to silicon come from water or not.

The most energetic favored product **4** can be seen as an OH derivative of SiH_4 as well as a SiH_3 derivative of H_2O. It can be expected that two molecules of **4** will further react to each other or to other H_2O or SiH_4 via a similar route as SiH_4 reacts with H_2O. The details of the possible further reactions are important to reveal mechanisms governing the sol−gel process. In the present work, our intention is not to study the larger and more complicated systems. Instead, we focus on the initial reaction stage of the SiH_4/H_2O system, to see what happens providing more energy to the system.

Part II: Pathways from SiH_4-H_2O (1) to OH or SiH_3 Radicals. Complexes containing Si−O or Si−OH bonds are found to be responsible for optic properties of porous silicon material both in manufacture processing and product application.[32−38] It is thus desirable to include electronic excited states in the reaction pathways of the SiH_4/H_2O system.

With energy of 87.03 kcal/mol, one of the hydrogen atoms attached to silicon in **1** can dissociate as shown by triplet state $H-SiH_3-H_2O\_3$ (**10**), leaving SiH_3-H_2O (**11**), a loose complex

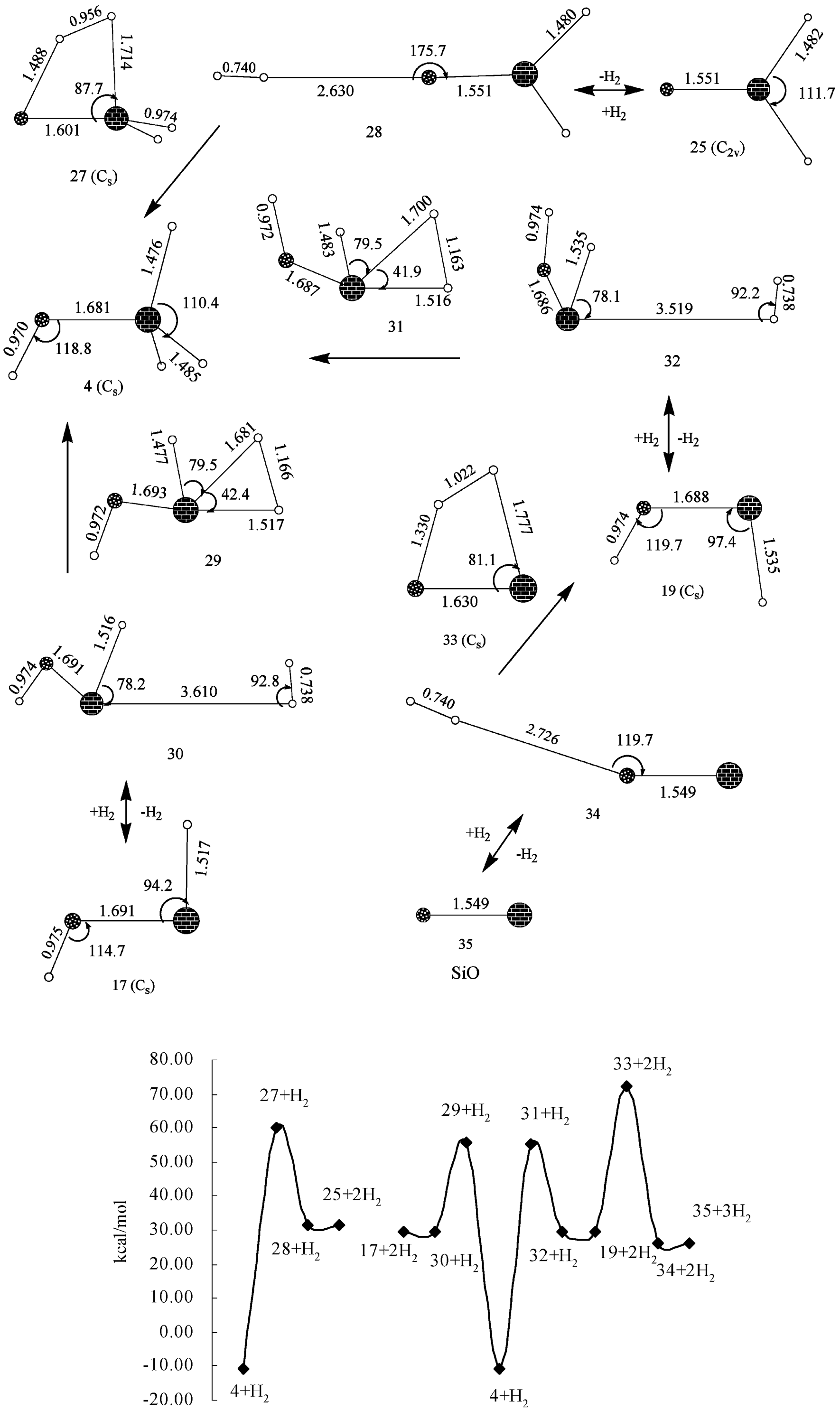

Figure 4. Species involved in H_2 elimination from SiH_3OH (**4**). Bond lengths are in Å, and angles are in degrees. The species beside arrows are transition states or H_2. The direction of arrows is toward energy descent. The relative energy of SiH_4-H_2O (**1**) is 0.00 kcal/mol. The symmetry of the species is indicated in parentheses but C_1 is omitted.

formed between molecule H_2O and radical SiH_3. SiH_3 is not a good attractor toward H_2O; the binding energy of SiH_3 and H_2O is only 0.87 kcal/mol, compared to the compact structure of **6** and the binding energy of 11.04 kcal/mol between SiH_2 and H_2O. Furthermore, the dipole moments of **1** and **11** are close to the value of isolated H_2O, whereas for **6**, the dipole moment is double the value of H_2O, indicating the larger electron-transfer effect in **6** than in **1** and **11**.

With energy of 112.06 kcal/mol, one of the hydrogen atoms attached to oxygen in **1** can dissociate as shown by a triplet state SiH_4-HO-H_3 (**14**), leaving SiH_4-HO (**13**), a loose complex formed between radical OH and molecule SiH_4. The binding energy is 0.54 kcal/mol, indicating the very small interaction between the two fragments.

The two H eliminated products **11** and **13** can convert to each other through H transfer between silicon and oxygen, as shown by H bridged transition state SiH_3-H-OH_TS (**12**). The barrier is 31.91 kcal/mol relative to **11**. Comparing the two processes, forming an OH radical is more energy demanding than forming a SiH_3 radical. Because the remaining radical−molecule interac-

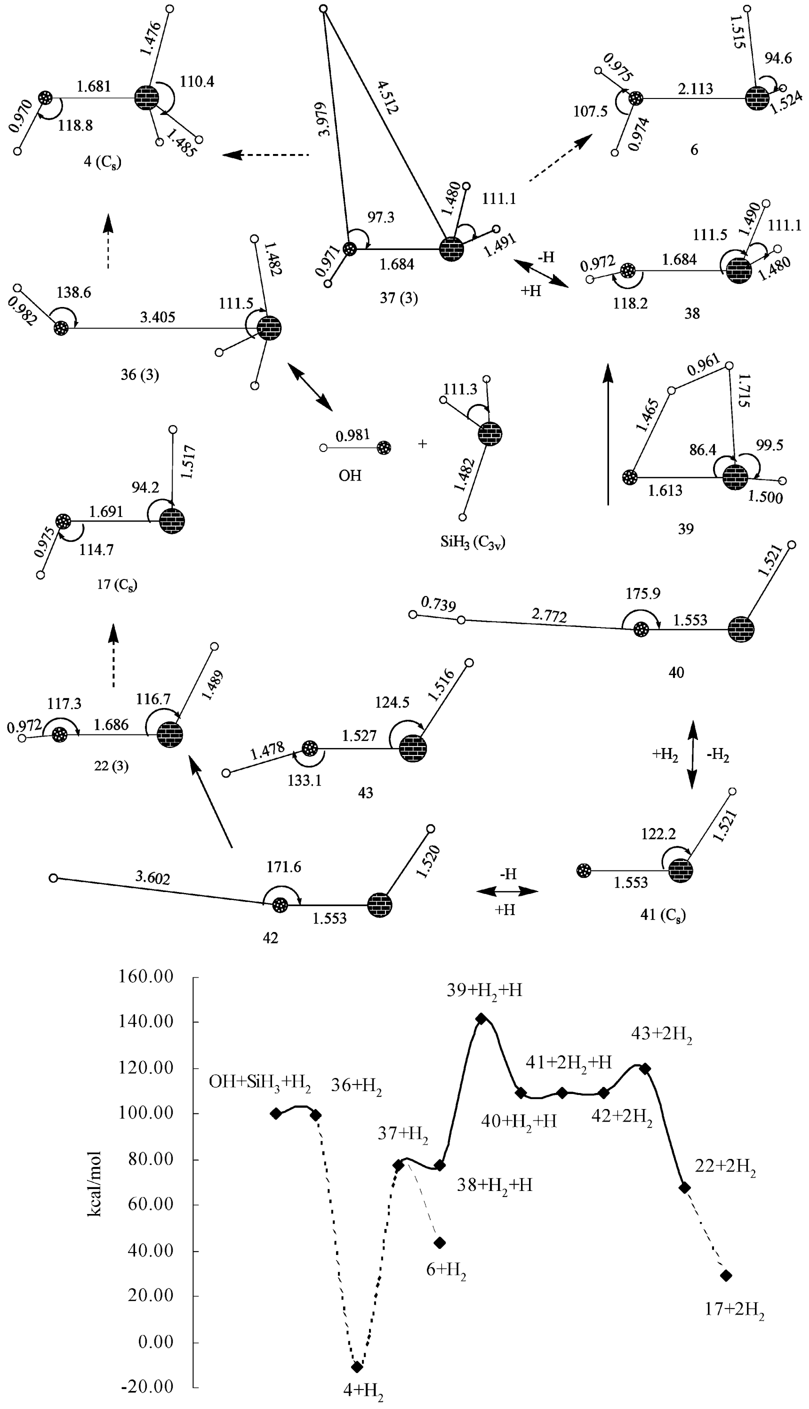

Figure 5. Species involved in H and OH elimination from SiH_3OH (**4**). Bond lengths are in Å, and angles are in degrees. The species beside arrows are transition states, H_2, or H. The direction of arrows is toward energy descent. The dashed lines or arrows indicate triplet−singlet transitions. The relative energy of $SiH_4{-}H_2O$ (**1**) is 0.00 kcal/mol. in parentheses, triplet species are labeled “3” and symmetry of the species are indicated except for C_1.

tion after either process is weak, there is no reason to infer that SiH_4 or H_2O mono-atomic-dissociation is helped by each other. In the presence of a H atom, both radicals **11** and **13** associate with H readily into **1**, so they are too transient to be observed without special trapping techniques.

In calculating the high spin species involved in this part, negligible spin contaminations are encountered as can be seen from the corresponding $\langle S^2 \rangle$ values.

Part III: Pathways from $SiH_2{-}H_2O$ (6) to SiH−OH (17), $SiH{-}OH_c$ (19), and $SiH_2{-}O$ (25). Starting from **6**, the system can eliminate a second H_2 through two dihydrogen bonded transition states, $SiH{-}H_2{-}OH\_TS$ (**15**) and $SiH{-}H_2{-}OH_c\_TS$ (**21**), resulting in two products $SiH{-}OH{-}H_2$ (**16**) and $SiH{-}OH_c{-}H_2$ (**20**), which are SiH−OH (**17**) and its cis isomers $SiH{-}OH_c$ (**19**) loosely associated with H_2. The barriers of the two processes are 22.22 and 22.54 kcal/mol relative to **6**. The energies of **16** and **20** are −14.04 and −13.94 kcal/mol relative to **6**. Despite the increase of the total energy to the system, the second H_2 elimination from **6** encounters a lower barrier than the first H_2 elimination from **1** and results in more stable species with less hydrogen content. There is essentially no energetic preference between the trans and cis processes and relevant products. The interconversion between **17** and **19**, as shown by

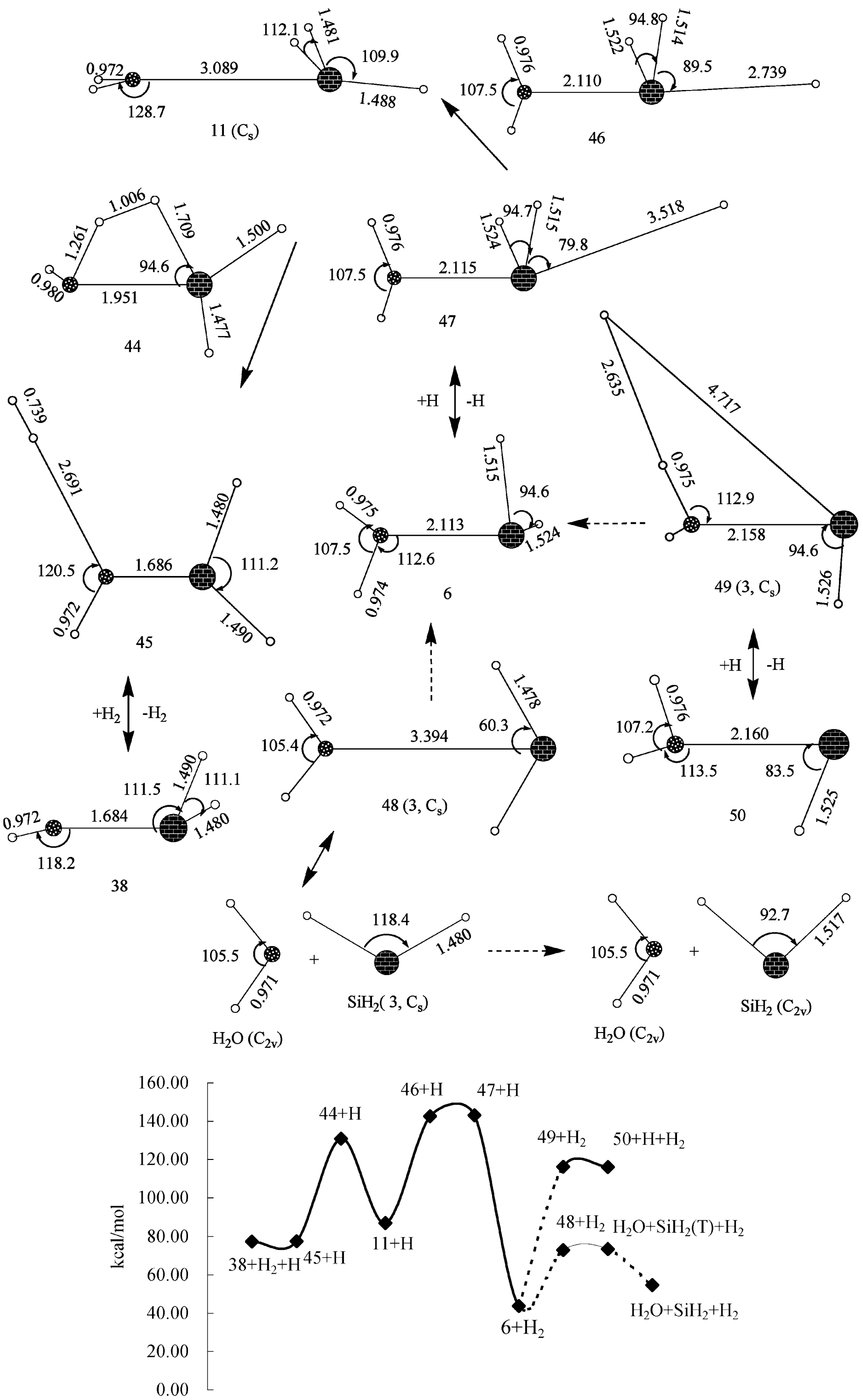

Figure 6. Species involved in H_2 or H elimination from SiH_3-H_2O (**11**) and dissociation of SiH_2-H_2O (**6**). Bond lengths are in Å, and angles are in degrees. The species beside arrows are transition states, H_2, or H. The direction of arrows is toward energy descent. The dashed lines or arrows indicate triplet−singlet transitions. The relative energy of SiH_4-H_2O (**1**) is 0.00 kcal/mol. In parentheses, triplet species are labeled "3" and symmetry of the species are indicated except for C_1.

transition state SiH−OH_TS (**18**), requires 7.82 kcal/mol energy, a barrier not large enough to make the two isomers separable species.

Compound **17** can be seen as an OH derivative of SiH_2. The OH group clearly stabilizes the two-coordinated silicon by donating negative charges. Over a much larger barrier of 58.60 kcal/mol, one of the hydrogen atoms can transfer from oxygen to silicon, as shown by transition state SiH−H−O_TS (**26**), resulting in silanone SiH_2−O (**25**), the silicon analogue of formaldehyde. In **25**, the Si−O and Si−H bonds are shortened and the four atoms are confined in a triangular planar structure, indicating that silanone has some sp^2 hybrid orbital character. The energy differences of isomers **25**, **17**, and **19** are within 1−2 kcal/mol and essentially agree with more accurate calculations.[39] Starting from **6**, it is easier to obtain **17** or **19** than **25**. Both **17** (**19**) and **25** can be excited to triplet states SiH−OH_3 (**22**) and SiH_2−O_3 (**24**). The triplet−singlet gap is 38.43 kcal/mol between **22** and **17** and 57.86 kcal/mol between **24** and **25**, both within visible region of photoluminescence. At the triplet state, the atoms are not confined in one plane for both species. The Si−O bond shortened from **17** to **22**, whereas it lengthened from **25** to **24**. Over a barrier of 19.54 kcal/mol,

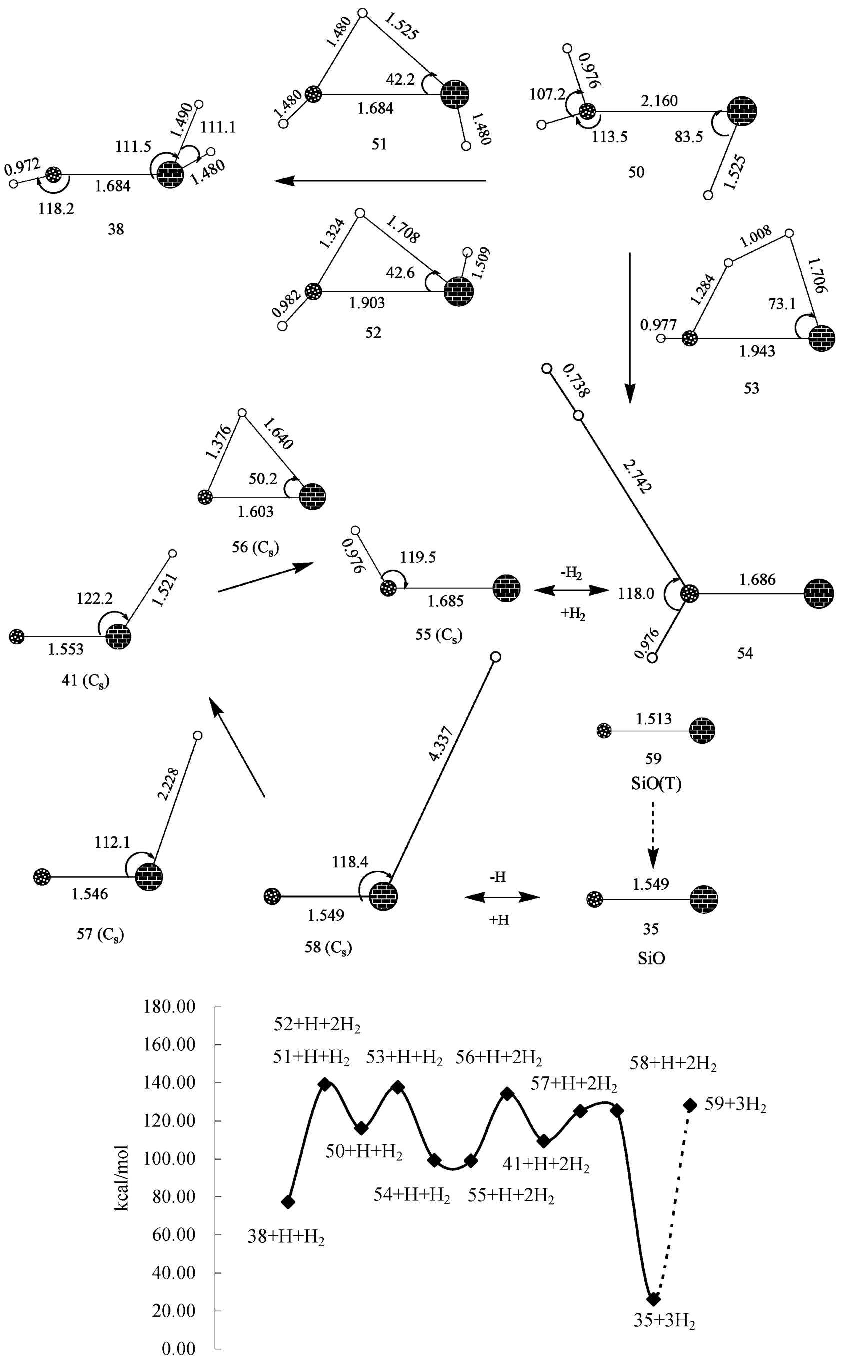

Figure 7. Species involved in isomerization, H and H_2 elimination from radical SiH_2-OH (**38**). Bond lengths are in Å, and angles are in degrees. The species beside arrows are transition states, H_2, or H. The direction of arrows is toward energy descent. The dashed lines or arrows indicate triplet−singlet transitions. The relative energy of SiH_4-H_2O (**1**) is 0.00 kcal/mol. The symmetry of the species is indicated in parentheses but C_1 is omitted.

the conversion from **24** to the more stable **22** can be realized, much easier than the conversion at the singlet state. The triplet transition state is SiH−H−O_3_TS (**23**), structurally very close to the singlet transition state **26** except that the C_s symmetry is broken. In calculating the structure and energy of triplet species in this part, no serious spin contamination is encountered, as can be seen from the corresponding $\langle S^2 \rangle$ values.

Part IV: Pathways from SiH_3OH(4) to SiH−OH (17), SiH−OH_c (19), and SiH_2−O (25) and from 19 to SiO (35). Silanol **4** is the most probable product since its formation stabilizes the total system. Under elevated temperature, however, hydrogen elimination can also take place from **4**. One way is through a dihydrogen bonded transition state SiH_2-H_2-O_TS (**27**). The activation energy is 70.76 kcal/mol relative to **4**. The product is SiH_2-O-H_2 (**28**), a molecular combination of SiH_2-O(**25**) and H_2. Being an OH derivative of SiH_4, compound **4** can eliminate H_2 in a similar way as SiH_4 dissociating into SiH_2 and H_2. With an activation energy of 66.62 or 66.07 kcal/mol relative to **4**, the dissociation can proceed along two ways as shown by transition states H_2−SiH−OH_TS (**29**) and H_2−SiH−OH_c_TS (**31**), resulting in H_2−SiH−OH (**30**) and H_2−SiH−OH_c (**32**), the molecular combination of **17** and **19** with H_2. There is no preference between the trans and cis process and products. It is quite difficult to judge through which way the second H_2 elimination really takes place. Starting from **6**, the activation energy is smaller than that starting from **4**; however, the total system needs more energy to reach the transition states.

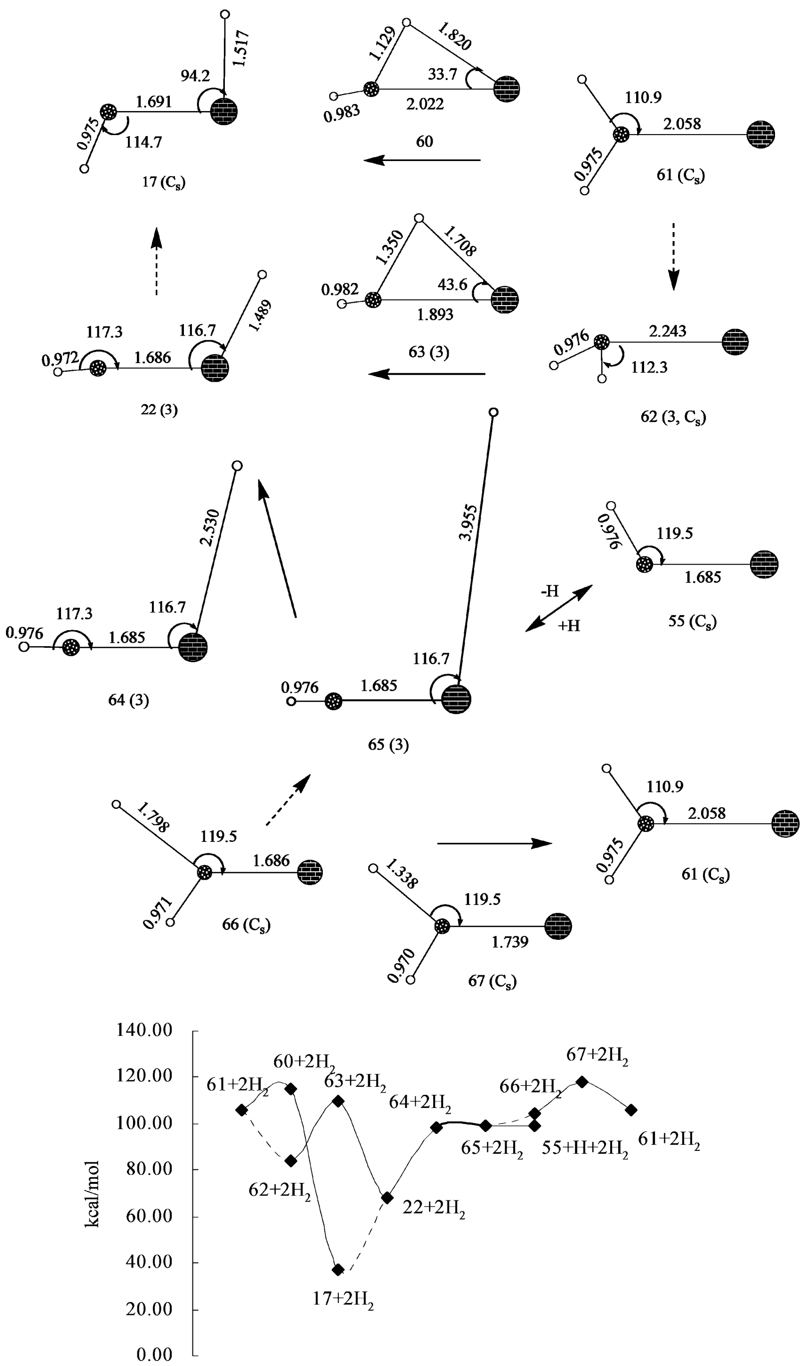

Figure 8. Species involved in isomerization, H elimination from SiH−OH(**17**). Bond lengths are in Å, and angles are in degrees. The species beside arrows are transition states or H. The direction of arrows is toward energy descent. The dashed lines or arrows indicate triplet−singlet transitions. The relative energy of SiH_4−H_2O (**1**) is 0.00 kcal/mol. In parentheses, triplet species are labeled "3" and symmetry of the species are indicated except for C_1.

Because the two hydrogen atoms in **19** are in the cis position, they can associate into a dihydrogen bonded transition state Si−H_2−O_TS (**33**), resulting in SiO−H_2 (**34**), the molecular combination of silicon monoxide SiO (**35**) and H_2. For the total system, the third H_2 elimination is not the most energy demanding process. The energy of **33** plus two H_2 is 72.20 kcal/mol relative to **1**, and the energy of the product **35** plus three H_2 is 26.07 kcal/mol relative to **1**, indicating SiO is quite a stable species and relatively easy to be produced during thermal reaction between SiH_4 and H_2O.

Part V: Pathways from SiH_3OH (4) to SiH_2−OH (38) and HSiO (41). Similar to SiH_4 in **10**, silanol **4** is able to eliminate either one H atom or an OH radical as shown by triplet states SiH_3−OH_3 (**36**) and H−SiH_2−OH_3 (**37**). It is relatively easier for **4** to eliminate an H atom than a OH radical. The energies of **36** and **37** are 110.62 and 88.14 kcal/mol relative to **4**. It can be seen that **36** is a loose association of OH and SiH_3 radicals. From **37**, two possibilities exist. First, the H associates with oxygen in **37**, resulting in **6**. Second, the H fully dissociates, leaving SiH_2−OH (**38**), an OH derivative of radical SiH_3. Providing 141.76 kcal/mol energy to the system or over a barrier of 64.48 kcal/mol, a H_2 molecule can dissociate from **38** through the dihydrogen bonded structure as shown by transition state SiH−H_2−O_TS (**39**). The product HSiO−H_2 (**40**) is a loose combination of radical HSiO (**41**) and H_2. The energy of **40** is 32.31 kcal/mol relative to **38**. Another way toward **41** starts from **22**, the triplet state of **17**. The OH group dissociates one H as shown by transition state HSiO−H_TS_3 (**43**) and product HSiO−H_3 (**42**), which is a loose combination of **41** and H atom. The barrier for **42** to go to **22** is 10.19 kcal/mol. As a result, although the system requires more energy to produce **41** than **38**, the smaller radical **41** is more likely observed, because upon formation, it can be trapped between two barriers. In contrast, the radicals OH, SiH_3, and **38** are more transient since they all fall back to **4** without barriers if H atom is present.

In calculating the triplet and doublet species involved in this part, no serious spin contamination are encountered. The largest $\langle S^2\rangle$ value is 2.180 for the triplet transition state **43**.

Part VI: Pathways from SiH_3−H_2O (11) to SiH_2−OH (38) and from SiH_2−H_2O (6) to SiH−H_2O (50) or SiH_2. The weakly associated radical−molecule complex **11**, if not separated to H_2O and SiH_3, can eliminate H_2 or H and produce species with a stronger Si−O bond. Over a barrier of 44.01 kcal/mol, the H_2 elimination takes place through dihydrogen bonded transition state SiH_2−H_2−OH_TS (**44**), producing SiH_2−OH−H_2 (**45**), a loose combination of **38** and H_2. Compared with H dissociation from **4**, the barrier from **11** to **38** is smaller, but the system requires more energy to reach **44**. The energy of **45** is −9.54 kcal/mol relative to **11**. If a H atom is not present nearby, we can expect the transient presence of **38** because of the barrier for the reverse reaction from **45** to **11**. However, if H is around, it can associate with **38** into **4** as indicated in Part V.

Providing 142.58 kcal/mol energy to the system, one of the H atoms associated with silicon in **11** can eliminate as shown by doublet transition state H−SiH_2−H_2O_TS (**46**), resulting in H−SiH_2−H_2O (**47**), a loose combination of **6** and H. The energy of **46** is very close to **47**, indicating this is an energy rising process and the reversed reaction from **47** to **11** proceeds without barrier. If the H atom fully dissociated from **47** associates with another H into H_2, the system's energy drops as **6** forms.

Starting from **6**, dissociation into two fragments SiH_2 and H_2O can happen via singlet−triplet state excitation. Providing 29.21 kcal/mol energy to **6**, it can be excited to triplet state SiH_2−H_2O_3 (**48**). The SiH_2 and H_2O groups in **48** are only weakly bonded. The dipole moment of **48** is very close to that of H_2O, whereas the dipole moment of **6** is double the value of H_2O. Comparing the structures of triplet and singlet states of SiH_2, we guess that the lone electron pair attached to Si may separate at triplet state SiH_2(T) and make it a SiH_4 like species with two single electrons in place of two Si−H bonds. In **48**, the SiH_2 group is actually in triplet state, so it cannot accept electron donation from oxygen and forming a dative bond with H_2O. The singlet−triplet gap of SiH_2 is 18.71 kcal/mol. Alternatively, providing 72.68 kcal/mol energy to **6**, it can be excited to another triplet state H−SiH−H_2O_3 (**49**). This is a loose combination of radical SiH−H_2O (**50**) and H. From the compact structure and large dipole moment of **50**, it can be inferred that the Si−O bond in **50** is dative in nature. The spin contaminations for the triplet and doublet species are small in this part. The most contaminated $\langle S^2\rangle$ value is 0.792 for doublet transition state **46**.

Part VII: Pathways from SiH_2−OH (38) to SiH−H_2O (50), HOSi (55), HSiO (41), and SiO (35). Providing 139.25 or 140.08 kcal/mol to the total system, radical **38** can isomerize to SiH−H_2O (**50**) by H transfer from Si to O as shown by transition states SiH−H−OH_c_TS (**51**) and SiH−H−OH_TS (**52**). The structure of **51** differs from **52** in the orientation of the O−H and Si−H bonds. Compound **50** is a molecular−radical combination between H_2O and SiH. Its energy is 38.93 kcal/mol relative to **38**. The large dipole moment of **50** shows it can be regarded as a dative complex of H_2O and SiH radical. Over a barrier of 21.53 kcal/mol, a H_2 molecule can eliminate from **50** as shown by transition state Si−H_2−OH_TS (**53**), resulting in SiOH−H_2 (**54**), a molecular combination of HOSi (**55**) and H_2. The energy of **55** is −10.23 kcal/mol relative to **41**. Thus, HOSi is more stable than its isomer HSiO. The interconversion between **41** and **55** has a barrier of 24.99 kcal/mol relative to **41** as shown by transition state Si−H−O_TS (**56**). The Si−H bond in **41** is not very strong. Besides isomerization, the radical **41** can dissociate a H atom over a barrier of 15.82 kcal/mol as shown by transition state H−Si−O_TS (**57**) and product H−SiO (**58**). If two eliminated H atoms associates into H_2, the system falls to **35** + $3H_2$.

Providing 102.23 kcal/mol energy, SiO(**35**) can be excited to triplet state SiO(T)(**59**). The Si−O bond shortens from **35** to **59** despite the energy rise from singlet to tiplet. The spin contamination is not serious for **59**.

Part VIII: Pathways from SiH−OH (17) to Si−H_2O (61) and HOSi (55). Compound **17** or its cis isomer **19** is the stable species containing two H atoms. Besides interconversion with another stable isomer **25** by transferring a H atom from oxygen to silicon, it can also convert to Si−OH_2 (**61**) by transferring a H from silicon to oxygen as shown by transition state Si−H−OH_TS (**60**). The later process, however, is more energy demanding. The energy of the product **61** is 68.59 kcal/mol and the barrier is 77.62 kcal/mol relative to **17**. The structure of **61** looks like a complex formed between H_2O and the Si atom. The four composing atoms in **61** are almost (not exactly) in a plane. The triplet state of the complex, Si−H_2O_3 (**62**), is 21.93 kcal/mol more stable than **61**. Comparing singlet state **61**, the Si−O bond in **62** is longer and the four atoms are clearly not in one plane, indicating the atom−molecule interaction character of the complex. The pathways started from **62** can thus interpret the mechanism of reaction between the silicon atom and the water molecule. When H_2O interacts with Si to form **62**, two pathways leads the complex to **17**. First, it can be excited to **61**, which then goes to **17** through transition state **60**. Second, the H atom transfer can happen at triplet state through transition state H−OH_3_TS_3 (**63**), resulting in **22**, the triplet state of **17**. Because the energy of **63** is 5.49 kcal/mol lower than **60**, the second pathway is slightly favored energetically.

Providing 98.69 kcal/mol energy to the system, the H atom connected to Si in **22** can dissociate as shown by triplet transition state HOSi−H_3_TS (**64**), resulting in HSiO−H_3 (**65**), the weak combination of radical **55** and a H atom. Because the energies of **64** and **65** are very close, radical **55** can associate with a nearby H atom and goes back to **22** almost without a barrier. This is different from its isomer **41**, which can be trapped in a small energy valley as shown in Part V. As a result, although HSiO (**41**) is less stable than HOSi (**55**) in isolated form, the former may stay longer than the later. This kinetic reason may account for the experimental fact that HSiO instead of HOSi is observed.[40−42]

Over a barrier of 12.17 kcal/mol, one of the H atom attached to oxygen in **61** can dissociate as shown by transition state SiOH−H_TS (**67**). The product is SiOH−H (**66**), in which radical **55** and H are partially separated. It is remarkable that both **66** and **67** are at singlet state although atomic dissociation is involved. The triplet state of **66** is **65**, a loose combination of **55** and H. The triplet−singlet gap is, however, only 4.80 kcal/mol with the triplet state lying lower. No serious spin contaminations are encountered in calculating the doublet and triplet species involved in this part.

III. Concluding Remarks

Gas-phase reactions between SiH_4 and H_2O start from H_2 elimination via three possible ways, dihydrogen bonding, SiH_4 self-dissoication, or atomic dissociation. The most energetic favored process is through dihydrogen bonded transition state, producing silanol SiH_3OH with retention of configuration. More energy is required to obtain SiH_3OH via a dative bonded intermediate $SiH_2{-}H_2O$, formed between SiH_2 and H_2O, but the original configuration is converted. Providing more energy to the system, SiH_3OH and $SiH_2{-}H_2O$ can eliminate a second H_2, resulting in $SiH_2{-}O$, $SiH{-}OH$, and $Si{-}H_2O$. The triplet−singlet gap for these species is relatively small. Atomic H dissociation can happen at various stages but is more energetic demanding. The intermediate radicals $SiH_2{-}OH$, $SiH{-}H_2O$, HSiO, and HOSi can be produced transiently, among them, HSiO is relatively easier detected. The fully hydrogen eliminated SiO is quite stable and can be produced via several ways. H_2 elimination from $SiH{-}OH$ through dihydrogen bonded transition state is energetically favored.

References and Notes

(1) Dominguez, C.; Rodriguez, J. A.; Riera, M.; Llobera, A.; Diaz, B. *J. Appl. Phys.* **2003**, *93*, 5125.

(2) Gougousi, T.; Kelly, M. J.; Parsons, G. N. *Appl. Phys. Lett.* **2002**, *80*, 4419.

(3) Haraguchi, T.; Sugiura, O. *Jpn. J. Appl. Phys.* **1996**, *2 35*, L1290.

(4) Ceiler, M. F.; Kohl, P. A.; Bidstrup, S. A. *J. Electrochem. Soc.* **1995**, *142*, 2067.

(5) Niwano, M.; Terashi, M.; Shinohara, M.; Shoji, D.; Miyamoto, N. *Surf. Sci.* **1998**, *401*, 364.

(6) Weldon, M. K.; Queeney, K. T.; Chabal, Y. J.; Stefanov, B. B.; Raghavachari, K. *J. Vac. Sci. Technol. B* **1999**, *17*, 1795.

(7) Henderson, M. A. *Surf. Sci. Rep.* **2002**, *46*, 5.

(8) Esteve, A.; Chabal, Y. J.; Raghavachari, K.; Weldon, M. K.; Queeney, K. T.; Rouhani, M. D. *J. Appl. Phys.* **2001**, *90*, 6000.

(9) Klemm, E.; Seitz, M.; Scheidat, H.; Emig, G. *J. Catal.* **1998**, *173*, 177.

(10) Ohki, A.; Ohmi, T.; Date, J.; Kijima, T. *J. Electrochem. Soc.* **1998**, *145*, 3560.

(11) Moore, J. F.; Strongin, D. R. *Thin Solid Films* **1996**, *280*, 101.

(12) Krasnoslobodtsev, A. V.; Smirnov, S. N. *Langmuir* **2002**, *18*, 3181.

(13) Fung, C. A. F. K.; Burke, M. F. *J. Chromatogr. A* **1996**, *752*, 41.

(14) Wovchko, E. A.; Camp, J. C.; Glass, J. A.; Yates, J. T. *Langmuir* **1995**, *11*, 2592.

(15) Shimojima, A.; Umeda, N.; Kuroda, K. *Chem. Mater.* **2001**, *13*, 3610.

(16) Wen, J. Y.; Wilkes, G. L. *Chem. Mater.* **1996**, *8*, 1667.

(17) Ingall, M. D. K.; Honeyman, C. H.; Mercure, J. V.; Bianconi, P. A.; Kunz, R. R. *J. Am. Chem. Soc.* **1999**, *121*, 3607.

(18) Parikh, A. N.; Schivley, M. A.; Koo, E.; Seshadri, K.; Aurentz, D.; Mueller, K.; Allara, D. L. *J. Am. Chem. Soc.* **1997**, *119*, 3135.

(19) Peters, M. A.; Belu, A. M.; Linton, R. W.; Dupray, L.; Meyer, T. J.; Desimone, J. M. *J. Am. Chem. Soc.* **1995**, *117*, 3380.

(20) Boutevin, B.; GuidaPietrasanta, F.; Ratsimihety, A.; Caporiccio, G. *Main Group Met. Chem.* **1997**, *20*, 133.

(21) Akamatsu, Y.; Makita, K.; Inaba, H.; Minami, T. *Thin Solid Films* **2001**, *389*, 138.

(22) Perch, N. S.; Kisanga, P.; Widenhoefer, R. A. *Organometallics* **2000**, *19*, 2541.

(23) Pellerite, M. J.; Wood, E. J.; Jones, V. W. *J. Phys. Chem. B* **2002**, *106*, 4746.

(24) Okumoto, S.; Fujita, N.; Yamabe, S. *J. Phys. Chem. A* **1998**, *102*, 3991.

(25) Kudo, T.; Gordon, M. S. *J. Am. Chem. Soc.* **1998**, *12*, 11432.

(26) Ignatov, S. K.; Sennikov, P. G.; Ault, B. S.; Bagatur'yants, A. A.; Simdyanov, I. V.; Razuvaev, A. G.; Klimov, E. J.; Gropen, O. *J. Phys. Chem. A* **1999**, *103*, 8328.

(27) Ignatyev, I. S.; Schaefer, H. F. *Organometallics* **2001**, *20*, 3113.

(28) Peng, C. Y.; Ayala, P. Y.; Schlegel, H. B.; Frisch, M. J. *J. Comp. Chem.* **1996**, *17*, 49.

(29) Frisch, M. J.; Trucks, G. W.; Schlegel, H. B.; Scuseria, G. E.; Robb, M. A.; Cheeseman, J. R.; Zakrzewski, V. G.; Montgomery, J. A., Jr.; Stratmann, R. E.; Burant, J. C.; Dapprich, S.; Millam, J. M.; Daniels, A. D.; Kudin, K. N.; Strain, M. C.; Farkas, O.; Tomasi, J.; Barone, V.; Cossi, M.; Cammi, R.; Mennucci, B.; Pomelli, C.; Adamo, C.; Clifford, S.; Ochterski, J.; Petersson, G. A.; Ayala, P. Y.; Cui, Q.; Morokuma, K.; Malick, D. K.; Rabuck, A. D.; Raghavachari, K.; Foresman, J. B.; Cioslowski, J.; Ortiz, J. V.; Stefanov, B. B.; Liu, G.; Liashenko, A.; Piskorz, P.; Komaromi, I.; Gomperts, R.; Martin, R. L.; Fox, D. J.; Keith, T.; Al-Laham, M. A.; Peng, C. Y.; Nanayakkara, A.; Gonzalez, C.; Challacombe, M.; Gill, P. M. W.; Johnson, B. G.; Chen, W.; Wong, M. W.; Andres, J. L.; Head-Gordon, M.; Replogle, E. S.; Pople, J. A. *Gaussian 98*, revision A.7; Gaussian, Inc.: Pittsburgh, PA, 1998.

(30) Jasinski, J. M.; Becerra, R.; Walsh, R. *Chem. Rev.* **1995**, *95*, 1203.

(31) Hu, S. W.; Wang, Y.; Wang, X. Y. Chu, T. W. Liu, X. Q. *J. Phys. Chem. A* **2003**, *107*, 2954.

(32) Zhang, M.; Ciocan, E.; Bando, Y.; Wada, K.; Cheng, L. L.; Pirouz, P. *Appl. Phys. Lett.* **2002**, *80*, 491.

(33) Chang, H. J.; Chen, Y. F.; Lin, H. P.; Mou, C. Y. *Appl. Phys. Lett.* **2001**, *78*, 3791.

(34) Gole, J. L.; Dixon, D. A. *Phys. Rev. B* **1998**, *57*, 12002.

(35) Yao, B. D.; Shi, H. Z.; Zhang, X. Y.; Zhang, L. D. *Appl. Phys. Lett.* **2001**, *78*, 174.

(36) Zhou, F. L.; Head, J. D. *J. Phys. Chem. B* **2000**, *104*, 9981.

(37) Gole, J. L.; Dudel, F. P.; Grantier, D.; Dixon, D. A. *Phys. Rev. B* **1997**, *56*, 2137.

(38) Seals, L.; Dudel, F.; Grantier, D.; Gole, J. L.; Bottomley, L. A. *J. Phys. Chem. B* **1997**, *101*, 8860.

(39) Martin, J. M. L. *J. Phys. Chem. A* **1998**, *102*, 1394.

(40) Izuha, M.; Yamamoto, S.; Saito, S. *J. Mol. Struct.* **1997**, *413*, 527.

(41) Koput, J. *J. Phys. Chem. A* **2002**, *106*, 12067.

(42) Yamaguchi, Y.; Xie, Y. M.; Kim, S. J.; Schaefer, H. F. *J. Chem. Phys.* **1996**, *105*, 1951.